JACS
JOURNAL OF THE AMERICAN CHEMICAL SOCIETY

Article

pubs.acs.org/JACS

# Efficient Subnanometric Gold-Catalyzed Hydrogen Generation via Formic Acid Decomposition under Ambient Conditions

Qing-Yuan Bi, Xian-Long Du, Yong-Mei Liu, Yong Cao,* He-Yong He, and Kang-Nian Fan

Department of Chemistry, Shanghai Key Laboratory of Molecular Catalysis and Innovative Materials, Fudan University, Shanghai 200433, P. R. China

Supporting Information

**ABSTRACT:** Formic acid (FA) has tremendous potential as a safe and convenient source of hydrogen for sustainable chemical synthesis and renewable energy storage, but controlled and efficient dehydrogenation of FA by a robust solid catalyst under ambient conditions constitutes a major challenge. Here, we report that a previously unappreciated combination of subnanometric gold and an acid-tolerant oxide support facilitates the liberation of CO-free $H_2$ from FA. Applying an ultradispersed gold catalyst comprising TEM-invisible gold subnanoclusters deposited on zirconia to a FA-amine mixture affords turnover frequencies (TOFs) up to 1590 per hour and a turnover number of more than 118 400 at 50 °C. The reaction was accelerated at higher temperatures, but even at room temperature, a significant $H_2$ evolution (TOFs up to 252 $h^{-1}$ after 20 min) can still be obtained. Preliminary mechanistic studies suggest that the reaction is unimolecular in nature and proceeds via a unique amine-assisted formate decomposition mechanism on Au−$ZrO_2$ interface.

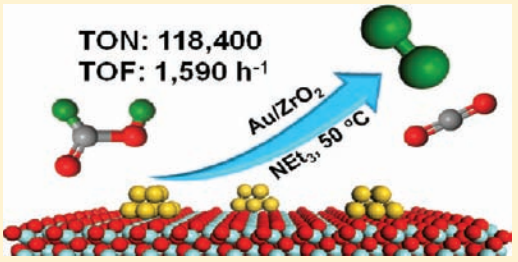


## INTRODUCTION

Hydrogen, an essential reagent for chemical and petrochemical industries, has been considered as one of the best candidates to satisfy the increasing demands for an efficient and clean energy supply.[1] Controlled storage and release of hydrogen are the widely known technological barriers in the fuel cell based hydrogen economy.[2] Recently, formic acid (FA), which is one of the major products formed in biomass processing and also accessible via a variety of chemical processes based on hydrolysis of methyl formate or $CO_2$ hydrogenation,[3a−c] was identified as a safe and convenient hydrogen carrier in fuel cells designed for portable use.[1b−d,3d,e] Hydrogen stored in FA can be released in situ on demand by catalytic dehydrogenation (HCOOH → $H_2$ + $CO_2$), with varied low levels of CO, generally produced by FA dehydration (HCOOH → $H_2O$ + CO), being coliberated as an undesirable byproduct. For the subsequent conversion of hydrogen into electrical energy, the CO impurity in the hydrogen gas must be strictly controlled.[4] Although FA has been widely used as a cheap and readily available hydrogen source in liquid-phase transfer reduction reactions,[5] a facile and selective evolution of an ultrapure $H_2$ gas (CO < 5 ppm) from FA decomposition under ambient conditions has proven to be extremely difficult. Hence, the successful development of an excellent protocol that can facilitate efficient and clean FA dehydrogenation at room temperature is of high actual interest.

In spite of the tremendous research efforts in the field of FA decomposition for $H_2$ generation, the number of catalysts that have prominent activity under practical and convenient conditions is still limited. The most effective catalyst system developed to date is a Ru−phosphine complex, with which hydrogen can be efficiently released with a turnover number (TON) up to 5716 (within 3 h at 40 °C) from FA-amine mixtures at temperatures as low as 26 °C.[6] Moreover, it was shown that a specifically designed water-soluble Ru-TPPTS system can release pressurized $H_2$ (up to 750 bar) from aqueous solution of FA/sodium formate (9:1) at temperatures of 70−120 °C.[7] Most recently, Boddien et al. reported an elegant noble-metal-free dehydrogenation of FA at 80 °C in environmentally benign propylene carbonate using an iron-based molecular catalyst system.[8] Compared to the great progress being made in the FA dehydrogenation with homogeneous systems,[3d,e,6−8] there are scarcely available reports dealing with the heterogeneously catalyzed dehydrogenation of FA at temperatures below 70 °C.[9] Although decomposition of FA as a model reaction has been extensively studied over a great number of heterogeneous catalyst systems since the early 1910s,[10] the focus has been largely on the fundamental reaction mechanism rather than clean and sustainable $H_2$ generation.[9,11] To the best of our knowledge, few reusable heterogeneous catalysts have been reported that enable clean and efficient FA dehydrogenation under ambient conditions.

Interest in using supported gold nanoparticles (NPs) or nanoclusters (NCs) as a low-temperature catalyst for green and sustainable chemical synthesis has gained considerable attention over the past few years.[12] In parallel to the pioneering work by Iglesia et al. that well-dispersed Au species can selectively decompose gaseous FA at 80 °C,[10g] we recently

**Received:** February 21, 2012
**Published:** May 8, 2012

   dx.doi.org/10.1021/ja301696e | J. Am. Chem. Soc. 2012, 134, 8926−8933

reported that small Au NPs (approximately 1.8 nm) deposited on acid-tolerant zirconia ($Au/ZrO_2$) can promote a facile hydrogen-independent transformation of aqueous bioderived levulinic acid (LA) and FA streams into γ-valerolactone (GVL),[13] a sustainable and highly versatile intermediate that has attracted tremendous interest for conversion of lignocellulosic biomass into fuels and valuable chemicals.[2b,c] The essential role of supported gold is to facilitate rapid and selective decomposition of FA to produce a hydrogen stream at 120–180 °C, thereby enabling a highly efficient reduction of LA without requiring an external source of hydrogen. We have now discovered a new generation of gold catalyst comprising TEM-invisible subnanometric gold clusters supported on $ZrO_2$ capable of dehydrogenating a FA-amine mixture under ambient conditions. This low-temperature FA decomposition method, using an easily handled and robust heterogeneous gold catalyst composed of ultrasmall Au NCs dispersed on $ZrO_2$, can make a significant contribution not only to disclose the intrinsic catalytic potential of gold but also to establish a more practical and convenient $H_2$ production process of great industrial importance.

## RESULTS AND DISCUSSION

Following our previous results in Au-catalyzed FA-mediated LA conversion,[13] we initially examined the decomposition of a highly acidic 10.5 M aqueous FA solution catalyzed by $Au/ZrO_2$ at 80 °C. Remarkably, the $Au/ZrO_2$ catalyst was found to be highly active and selective for FA dehydrogenation in acidic media, with an initial turnover frequency (TOF) of up to 550 $h^{-1}$ achievable for the exclusive formation of $H_2$ and $CO_2$ (Table S1, Supporting Information). Prompted by this result, we examined the gas evolution from aqueous FA in presence of $Au/ZrO_2$ at 40 °C. However, the reaction turned out to be extremely slow under this condition (Table S1, Supporting Information). With the aim to improve catalyst performance, we examined the use of various inorganic bases in various ratios, whereby we took into account recent findings by Laurenczy and Himeda et al.,[7,14] which showed a strong dependence of the catalyst activity and selectivity on the composition of aqueous FA. After a preliminary screening, we found that the use of HCOONa with FA/HCOONa ratio of 7:3 led to a significant increase of the reaction rate from 9 to 74 $h^{-1}$ at 40 °C (Figure S1, Supporting Information). The need for appreciable amounts of formate was in line with previous observations that the crucial formate dehydrogenation step during the transition-metal-catalyzed FA decomposition is highly sensitive to the concentration of formate ions.[7,14]

To optimize the reaction further, we turned our attention to the decomposition of FA and amine adducts, a useful compound material that has received tremendous attention in recent years as an efficient low-temperature hydrogen generation system wherein several homogeneous Ru- or Fe-based complexes bearing air-sensitive phosphine or terpyridine ligands were employed as the catalysts.[6,15] It should be emphasized that no reusable solid catalyst has yet been reported to be active and selective for this particular system at low temperature, despite the anticipated advantages in catalyst separation and processing. We were pleased to find that an efficient decomposition of a FA-amine mixture can be achieved by using the easily handled ligand-free solid $Au/ZrO_2$ catalyst at 40 °C. Additional experiments with various tertiary alkyl amines and varying ratios of amines to FA showed that the composition of the reaction medium was one of the key aspects in facilitating the desired $H_2$ evolution. In particular, the combination of FA and $NEt_3$ was found to be essential for achieving high activity in the Au-catalyzed FA dehydrogenation (Figure S2, Supporting Information). Notably, a 5:2 FA-$NEt_3$ azeotropic mixture (TEAF) gave the best results (Figure S3, Supporting Information). Thus, at 40 °C, $Au/ZrO_2$ can catalyze the decomposition of TEAF to produce $H_2$ with an initial TOF up to 250 $h^{-1}$ (Table 1, entry 1).

**Table 1. Study of Various Solid Catalysts for the Generation of $H_2$ via FA-$NEt_3$ Adducts Decomposition[a]**

$$HCOOH \xrightarrow[NEt_3]{cat., T} H_2 + CO_2$$

| entry | catalyst | metal (μmol) | $V_{gas}$ (mL) | TOF ($h^{-1}$)[b] | TON[c] |
|---|---|---|---|---|---|
| 1 | $Au/ZrO_2$ | 30.0 | 668 | 250 | 192 (451) |
| 2 | $Au/ZrO_2$ NCs | 30.0 | 2380 | 912 | 741 (1607) |
| 3[d] | $Au/ZrO_2$ NCs | 30.0 | 992 | 252 | 245 (670) |
| 4 | $Au/ZrO_2$ NCs | 3.75 | 300 | 923 | 748 (1621) |
| 5[e] | $Au/ZrO_2$ NCs | 3.75 | 270 | 799 | 621 (1458) |
| 6[f] | Ag@Pd/C | 30.0 | 80 | 49 | 38 (56) |
| 7[g] | $Au/Al_2O_3$ | 30.0 | 174 | 64 | 53 (117) |
| 8[h] | Pd–Au/C | 30.0 | 146 | 90 | 69 (102) |
| 9 | $Au/TiO_2$ | 30.0 | 566 | 226 | 175 (382) |
| 10 | $Au/TiO_2$ NCs | 3.75 | 168 | 559 | 406 (908) |
| 11 | $Au/SiO_2$ | 30.0 | 0 | — | — |
| 12 | Au/C | 30.0 | 0 | — | — |
| 13[i] | $Au/ZrO_2$ NCs | 3.75 | 553 | 1593 | 1318 (2990) |

[a]Reaction conditions: 5.0 mL scale of adducts (53.0 mmol FA, 21.2 mmol $NEt_3$), 40 °C, reaction time 3 h. [b]Initial TOF after 20 min. [c]TON for 1 h, numbers in parentheses refer to TON for 3 h. [d]Reaction performed at 25 °C. [e]The seventh reuse of $Au/ZrO_2$ NCs catalyst. [f]Ag@Pd/C prepared according to ref 9. [g]$Au/Al_2O_3$ prepared according to ref 10g. [h]Pd–Au/C prepared according to ref 11a. [i]Reaction performed at 50 °C.

Bearing in mind that particle size has proven especially influential for supported gold catalysts, we envisioned that dispersed Au NCs with improved metal dispersion could be more effective for $H_2$ production from TEAF. To explore this possibility, a new heterogeneous Au catalyst sample composed of ultrasmall Au NCs finely dispersed on $ZrO_2$ (denoted as $Au/ZrO_2$ NCs) was prepared by a careful regulation of the preparation conditions (see the Supporting Information for experimental details). To our delight, this catalyst gave much higher TOFs: up to 748 and 540 $h^{-1}$ after 1 and 3 h at 40 °C (Table 1, entry 4), respectively. Particularly noteworthy is that this Au catalyst gave an exceptional initial TOF up to 923 $h^{-1}$, which constitutes the highest activity ever reported for heterogeneously catalyzed FA decomposition. At temperature as low as 25 °C, $Au/ZrO_2$ NCs can also decompose FA with initial TOF of ca. 252 $h^{-1}$ (Table 1, entry 3). Moreover, a FA conversion of up to 94% can be readily obtained, even at 25 °C (Figure 1). Also of note is that in all catalytic experiments, only an ultratrace level of CO (<5 ppm, Figure S4 and Table S2, Supporting Information) has been detected in the evolved gaseous mixture. Thus, FA can be easily and efficiently


dx.doi.org/10.1021/ja301696e | J. Am. Chem. Soc. 2012, 134, 8926–8933

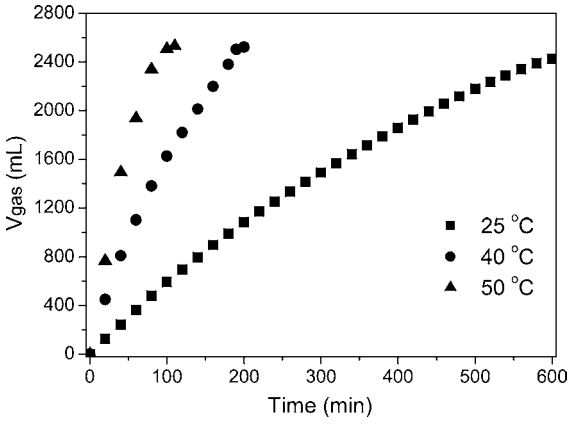


**Figure 1.** Kinetic traces for gas evolution via FA dehydrogenation catalyzed by Au/$ZrO_2$ NCs. Reaction conditions: 5.0 mL scale of TEAF adducts (53.0 mmol FA, 21.2 mmol $NEt_3$), 30.0 $\mu$mol Au.

converted into CO-free $H_2$-containing stream by ultradispersed Au, which is important for fuel cell applications.

The reaction did not proceed at all with Au-free $ZrO_2$ (Table S2, Supporting Information), showing that the presence of gold was essential for achieving high activity in the dehydrogenation of FA in TEAF. A comparison with palladium, platinum, ruthenium, rhodium, and iridium NPs supported on zirconia or activated carbon as reference catalysts showed that gold is uniquely active for selective FA decomposition compared with other noble metals (Table S2, Supporting Information). Note that previously reported solid catalysts, such as Ag@Pd/C,[9] $Au/Al_2O_3$,[10g] and Pd–Au/C[11a] showed only very low activities under the conditions as employed in this work (Table 1, entries 6–8). Since it has been shown that the choice of the underlying support plays an important role in gold catalysis, we also evaluated gold NPs supported on $TiO_2$, and the resultant catalyst was significantly less active for FA decomposition under similar reaction conditions (Table 1, entry 9). Meanwhile, gold supported on silica (Au/$SiO_2$) and activated carbon (Au/C) was completely ineffective for the desired reaction (Table 1, entries 11 and 12). These results indicate that both the noble metal and the nature of the support play important roles in the catalytic activity of FA decomposition. Among the various catalysts investigated in this study, ultrasmall Au NCs deposited on $ZrO_2$ (Au/$ZrO_2$ NCs) afford by far the best catalytic performance.

The high catalytic activity of Au/$ZrO_2$ NCs prompted a more detailed study, and several important features of the subnanometric Au-mediated hydrogen generation from FA have been elucidated. One notable advantage is that the hydrogen evolution rate at 40 °C did not depend on the $O_2$ concentration in the reaction atmosphere (Table S2, Supporting Information), thus offering practical and real advantages over existing technology or methods to establish a more convenient, readily available $H_2$ production process for micro fuel cell applications. Moreover, on addition of Au/$ZrO_2$ NCs into the TEAF mixture, the $H_2$ gas can be immediately generated without any induction period, in contrast to previously reported activities using Ru-based complexes.[6] In addition, the Au/$ZrO_2$ NCs catalyst was recoverable by simple filtration and proven robust even after seven reuses (Table 1, entry 5, and Figure S5, Supporting Information).[16] It was also found that the hydrogen evolution rate can be greatly enhanced at 50 °C (Table 1, entry 13, and Figure 1). The apparent activation energy ($E_a$) of this process was estimated to be 49.3 kJ $mol^{-1}$ (Figure S6, Supporting Information), which is lower than most of the previously reported heterogeneous catalyst systems for FA dehydrogenation.[10g] Furthermore, the reaction appears to be wholly unimolecular since decomposition of either HCOOD or DCOOH under identical conditions leads to exclusive formation of HD rather than a mixture of $H_2$, HD, and $D_2$ (Table 2). The most significant finding, however, was

**Table 2. Rate of $H_2$ Evolution, KIEs, and Isotope Distribution for Evolved Hydrogen Gas in Decomposition of FA Catalyzed by Au/$ZrO_2$ NCs[a]**

| | | | | fraction (mol %) | | |
|---|---|---|---|---|---|---|
| entry | FA | rate (mmol $min^{-1}$ $g_{Au}^{-1}$) | KIE[b] | $H_2$ | $D_2$ | HD |
| 1 | HCOOH | 52.1 | — | 100 | 0 | 0 |
| 2 | HCOOD | 30.6 | 1.7 | 0 | 0 | 100 |
| 3 | DCOOH | 20.0 | 2.6 | 0 | 0 | 100 |
| 4 | DCOOD | 11.6 | 4.5 | 0 | 100 | 0 |

[a]Reaction conditions: 5.0 mL scale of adducts (53.0 mmol FA, 21.2 mmol $NEt_3$), 3.75 $\mu$mol Au, 40 °C, reaction time 2 h. [b]KIE = rate (entry)/rate (entry $n$) ($n$ = 2–4).

that the present subnanometric Au-catalyzed FA dehydrogenation can proceed smoothly even at elevated pressures. The pressure of evolved gas may exceed 5.3 MPa (Figure S7, Supporting Information), with the FA decomposition being allowed to go to completion in a separate reaction performed in a closed vessel. This fact shows that the pressures in the system did not inhibit the reaction.

Having established that Au/$ZrO_2$ NCs are able to catalyze the generation of pressurized hydrogen at ambient conditions, we have explored the possibility to produce a continuous stream of practical applications by using the Au/$ZrO_2$ NCs-mediated FA dehydrogenation methodology. We have constructed a high-pressure device that allows a continuous addition of FA and the control of gas outflow under pressurized conditions. By maintaining a constant pressure of ca. 2.0 MPa inside the autoclave, the activity of the Au/$ZrO_2$ NCs sample at 50 °C could remain constant for more than 100 h, in which the TON approached up to 118 400 with an excellent average TOF of approximately 1184 $h^{-1}$ (Figure 2). Under continuous hydrogen production conditions as shown in Figure 2, the average rate of $H_2$ gas production was determined to be ca. 148

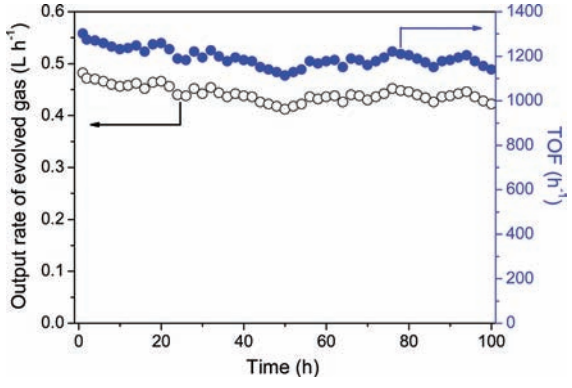


**Figure 2.** Continuous $H_2$ gas production using the Au/$ZrO_2$ NCs TEAF system. Reaction conditions: 10.0 mL scale of adducts (106.0 mmol FA, 42.4 mmol $NEt_3$), 7.5 $\mu$mol Au, 50 °C.


dx.doi.org/10.1021/ja301696e | J. Am. Chem. Soc. 2012, 134, 8926–8933

L $H_2$ $h^{-1}$ $g_{Au}^{-1}$. Such hydrogen output corresponds to a theoretical power density of 200 W $h^{-1}$ $g_{Au}^{-1}$ for energy generation.[6a,9,11a,17] Taking an operation efficiency of 60% and a typical energy requirement value of ca. 0.5−2.0 Wh for portable terminals, such as a cell phone in consideration, it turns out that 0.5−2.0 g of the present Au/$ZrO_2$ NCs catalyst would be sufficient to supply hydrogen for small proton exchange membrane (PEM) fuel cell devices.[18]

Although extensive mechanistic study has not yet been conducted, the decomposition of the transient Au-formate species formed by critical FA dissociation could be involved in the rate-determining step on the basis of kinetic isotope effect (KIE) measurements with HCOOD, DCOOH, and DCOOD (Table 2) as well as the indispensable role of $NEt_3$ in facilitating the reaction progress (Figure S3, Supporting Information). As depicted in Scheme 1, the key aspect of $NEt_3$ is to facilitate the

**Scheme 1. Possible reaction pathway for hydrogen evolution from the TEAF system over the Au/$ZrO_2$ NCs catalyst**

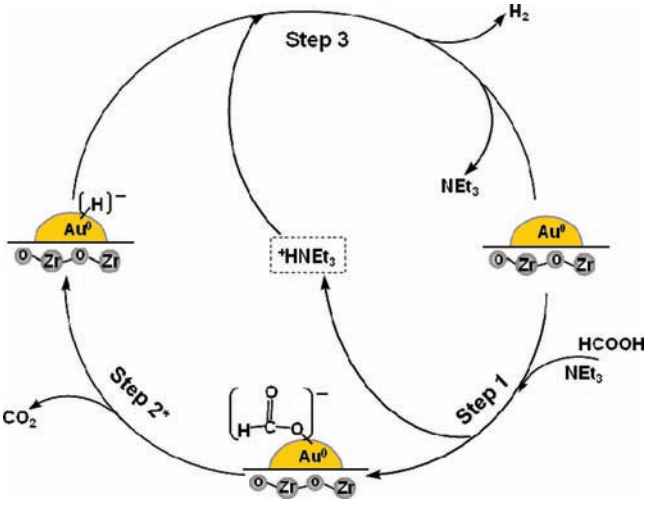


O−H bond cleavage as a proton scavenger, leading to the formation of a metal-formate species during the initial step of the reaction. The Au−formate complex may undergo further dehydrogenation, in association with the $^+HNEt_3$ species formed via the reaction of $NEt_3$ with FA, to produce molecular hydrogen along with $CO_2$ via a $\beta$-elimination pathway.[10g,19] Meanwhile, the exclusive formation of HD from HCOOD or DCOOH indicates that the final hydrogen desorption step is irreversible and also kinetically relevant, highlighting the feasibility of using renewable FA as a convenient in situ hydrogen source in place of molecular $H_2$ for sustainable and green organic synthesis. In the overall reaction for FA dehydrogenation, the cooperative action between ultrasmall Au clusters and $ZrO_2$ matrix plays an important role in leading to the crucial Au−formate activation under mild conditions.

A full characterization of the Au/$ZrO_2$ NCs sample was performed. From the X-ray photoelectron spectroscopic (XPS) data presented in Figure S8, Supporting Information, it can be seen that there is only metallic gold on the surface of the Au/$ZrO_2$ NCs catalysts.[20] The fact that no bands for $Au^+$ or $Au^{\delta+}$ can be seen from the diffuse reflectance infrared Fourier transform (DRIFT) spectra (Figure S9, Supporting Information) of adsorbed CO further confirm the exclusive presence of metallic Au species in this material. Whereas the surface Au/Zr atomic ratio (Table S3, Supporting Information) together with the DR UV−vis data (Figure S10, Supporting Information) unambiguously demonstrate that the gold dispersion in the Au/$ZrO_2$ NCs sample is distinctly higher than that for Au/$ZrO_2$, the identification of the ultrasmall Au clusters by TEM analysis was unsuccessful (Figure 3) for the Au/$ZrO_2$ NCs sample, apparently owing to the very fine nature of the Au species. Extended X-ray absorption fine structure (EXAFS) measurements have thus been carried out to clarify a possible structure of the metallic $Au^0$ species. However, no meaningful information can be obtained (not shown), possibly due to the poor contrast between gold and $ZrO_2$ support (in transmission mode) or the strong interference of fluorescent signal of $ZrO_2$ support (in fluorescent mode).[21] We then sought to use a low-temperature CO titration approach[22] to elucidate the intricate nature of the TEM-invisible Au species. Thanks to the method of pulse flow CO chemisorption at −116 °C, it has been possible to clarify the subnano nature of the Au species (approximately 0.8 nm, Table S4, see the Supporting Information for analysis details) through a careful quantitative estimation.

These results, together with the fact that markedly improved $H_2$ evolution can also be achieved with very small gold (approximately 1.1 nm) dispersed on titania (Table 1, entry 10), highlight the pivotal role of the subnanometric nature of Au clusters in facilitating the title reaction. It should be noted that such subnanoscale phenomenon is consistent with a previous observation by Iglesia et al.[10g] that highly dispersed TEM-invisible gold species on alumina show superior catalytic activity toward gas-phase FA dehydrogenation at 80 °C. To gain further information about the effect of Au particle size on catalytic activity, we compared Au/$ZrO_2$ NCs and Au/$ZrO_2$ for the room temperature (RT) CO oxidation, low-temperature (LT) water−gas shift (WGS) reaction and the title reaction (Figure 4). It is revealed that both the FA dehydrogenation and WGS reaction over Au/$ZrO_2$ NCs proceed much more rapidly than those for the Au/$ZrO_2$ sample. This is not unexpected given the above mechanistic study and generally accepted fact[10g] that a common formate-type intermediate could be involved for both FA dehydrogenation and LT-WGS reactions. The above results are however in sharp contrast to those that occurred for ambient CO oxidation, the most widely reaction investigated for supported gold catalysts. It turns out that the Au/$ZrO_2$ NCs sample can only deliver a very limited activity for RT CO oxidation, as opposed to the much higher activity as identified for the $ZrO_2$ supported Au NPs having diameters of ca. 1.8 nm.[23] It should be mentioned here that although the particle-size effect of Au has been extensively studied for CO oxidation, most studies have focused on the catalysts with a gold size above 2 nm.[24] To our knowledge, these results constituted the first and clear evidence of the reaction-dependent particle size effect in supported Au catalysts.

A further noteworthy finding of the present work is that apart from the gold particle size, the identity of the underlying support also plays an essential role in determining the catalytic performance of the final materials. Specifically, the combination of small size gold and $ZrO_2$ is found to be crucial to give an exceptionally active catalyst capable of facilitating the liberation of CO-free $H_2$ from FA under ambient conditions. Zirconia is a unique material of excellent thermal stability and chemical inertness, moreover, its surface possesses both acid−basic and redox functions.[25] As a result, $ZrO_2$ has attracted considerable recent attention as a support material as well as a catalyst. For a number of reactions,[26] the use of $ZrO_2$ as a support has been


dx.doi.org/10.1021/ja301696e | J. Am. Chem. Soc. 2012, 134, 8926−8933

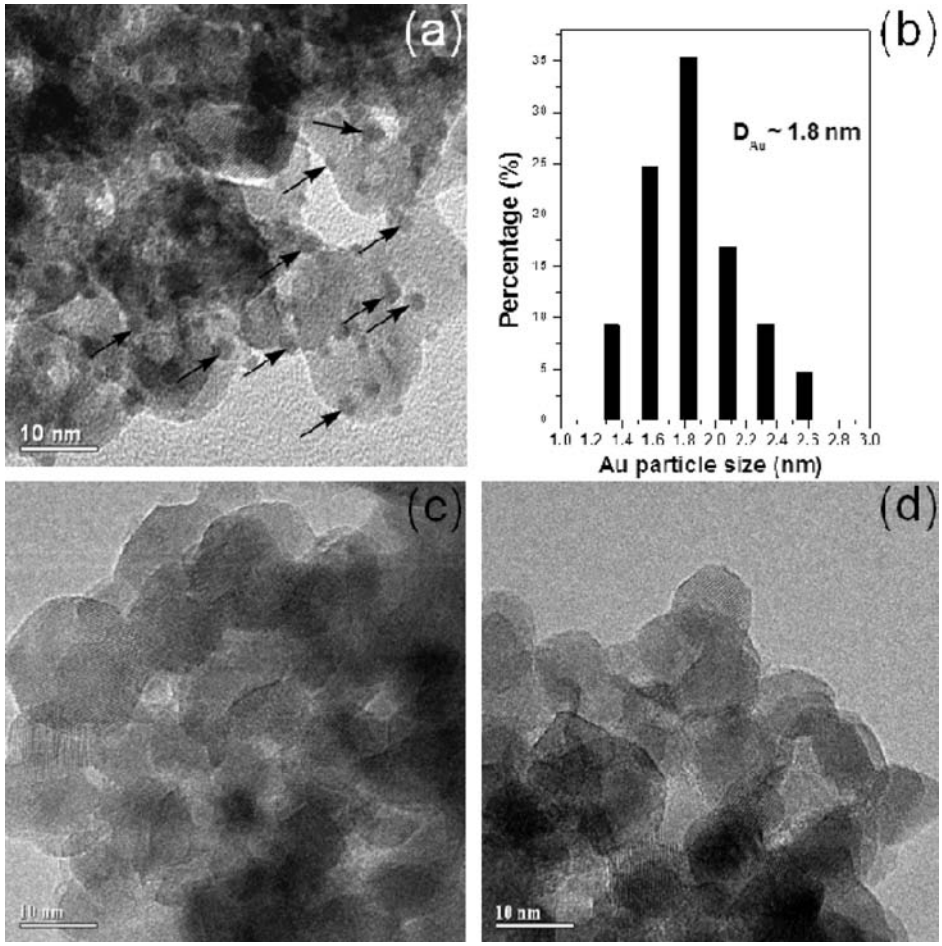


**Figure 3.** TEM images of (a) $Au/ZrO_2$ (with selected Au nanoparticles marked with arrows), (b) the gold particle size distribution on $Au/ZrO_2$, and (c) fresh and (d) used $Au/ZrO_2$ NCs.

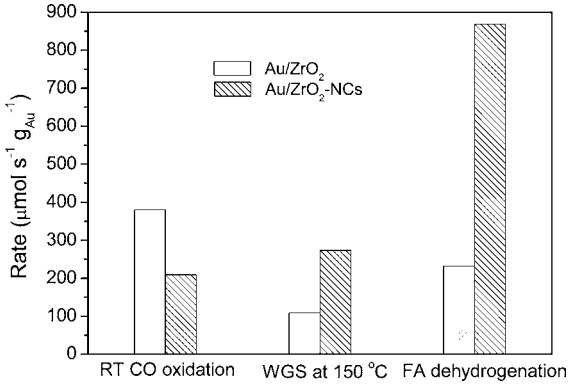


**Figure 4.** Comparison of reaction rate of $Au/ZrO_2$ and $Au/ZrO_2$ NCs for room temperature CO oxidation, LT-WGS and FA dehydrogenation (5.0 mL scale of adducts with 53.0 mmol FA and 21.2 mmol $NEt_3$, 3.75 $\mu$mol Au, 40 °C, reaction time 2 h). Reaction rate based on total Au.

reported to give improved activity and selectivity because of the amphoteric character of its surface nature. To clarify the origin of the enhanced FA decomposition activity achieved by using $ZrO_2$ as support, we have examined the effect of support on the interaction between HCOOD and several catalysts with similar mean Au particle sizes (ca. 2 nm) using time-resolved in situ IR (Figure 5). It is revealed that the H/D exchange reaction over $Au/ZrO_2$ occurred with much higher rates than that over other catalysts, which shows an excellent correlation with the catalytic data as reported in Table 1. Therefore, in line with the preliminary mechanistic insight as extracted from KIE studies, the fact that the amphoteric zirconia support can substantially facilitate crucial FA deprotonation appears to be a key factor for achieving high activity in the catalytic FA dehydrogenation.

## ■ CONCLUSIONS

In summary, for the first time, mild and selective dehydrogenation of FA/amine mixtures was demonstrated using ultradispersed subnanometric gold as catalysts. The reactions, catalyzed by Au subnanoclusters dispersed on acid-tolerant $ZrO_2$, proceed efficiently and selectively under ambient conditions, without the generation of any unwanted byproduct, such as CO, and with high TOFs/TONs. Moreover, the reactions proceed very well also at elevated pressures, as demonstrated for the cases of the continuous generation of a pressurized stream for $H_2$-based power generation, representing a significant step toward the practical development of formic acid as a viable storage medium for hydrogen that could be used in fuel cells or chemical synthesis. A unimolecular mechanism involving unique amine-assisted formate decomposition at the $Au-ZrO_2$ interface is supported by the exclusive formation of HD and the primary kinetic isotope effects measured from HCOOD or DCOOH dehydrogenation. Whereas the exceptional activity of subnanometric Au toward FA activation promises a new area of gold research, we


dx.doi.org/10.1021/ja301696e | J. Am. Chem. Soc. 2012, 134, 8926−8933

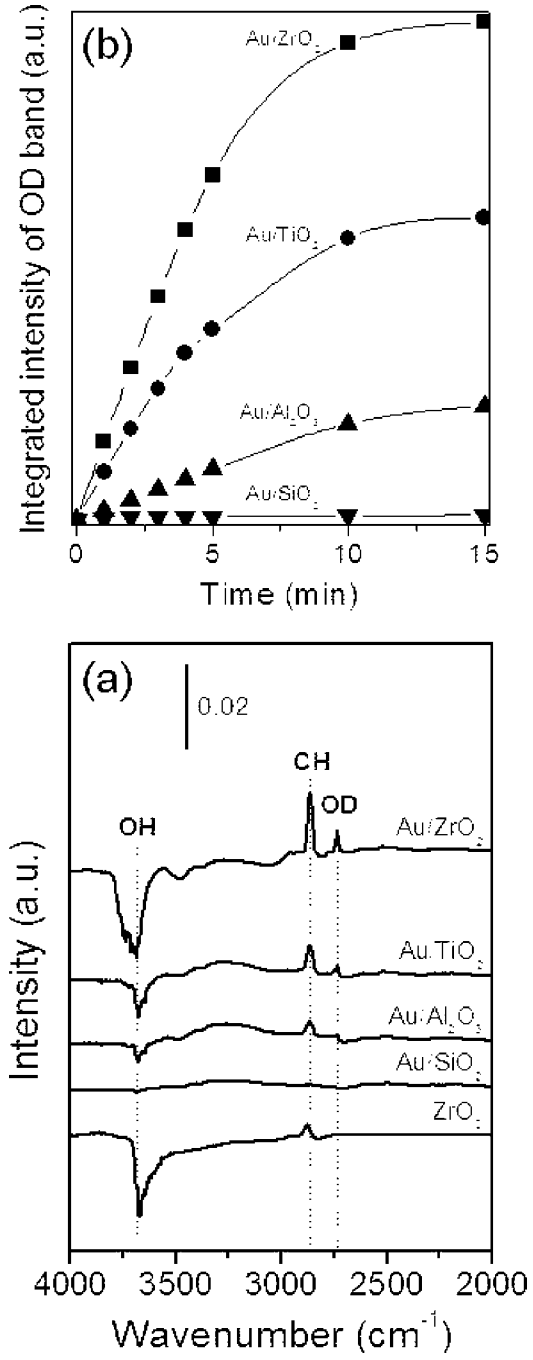


**Figure 5.** H/D exchange of HCOOD with surface OH groups of the catalysts at 60 °C. (a) DRIFT spectra recorded after a 15 min exposure to 2% HCOOD in He. (b) Integrated intensity of OD band with respect to exposure time. The fact that no OD band could be found in the bare $ZrO_2$ sample points to that the relevant FA deprotonation occurs exclusively at the metal−support interface.

anticipate that by a fine-tuning of the dispersed Au clusters at the subnano level, it is possible to design a new generation of advanced nanocatalyst systems that are important for sustainable energy production and chemical synthesis.

## EXPERIMENTAL SECTION

**Preparation of $ZrO_2$ Support.** $ZrO_2$ (specific surface area: 115 $m^2\ g^{-1}$, 56% monoclinic phase, and 44% tetragonal phase) powders were prepared by a conventional precipitation method following the reported procedure.[13] Briefly, 8.0 g zirconium oxychloride octahydrate ($ZrOCl_2{\cdot}8H_2O$) was dissolved in 200 mL deionized water, and the pH was adjusted to about 9.5 by dropwise addition of $NH_4OH$ (2.5 M) under stirring at room temperature. The resultant hydrogel was washed with deionized water until free of chloride ions after stirring for 8 h. The precipitate was then dried at 100 °C overnight followed by calcination at 400 °C in air for 2 h to obtain the final support.

**Preparation of Au/$ZrO_2$ Catalyst.** A modified deposition−precipitation (DP) procedure has been employed to prepare the Au/$ZrO_2$ sample.[13] Briefly, 2.0 g $ZrO_2$ powder was dissolved with desired amounts of aqueous solution of $HAuCl_4$ (100 mL, 1 mM), and the pH was adjusted to 9.0 by dropwise addition of 0.25 M $NH_4OH$ (CAUTION: the addition of $NH_4OH$ to $HAuCl_4$ solution could give rise to highly explosive fulminating gold). After 6 h of stirring at room temperature, the catalyst was washed five times with deionized water and separated by filtration. The samples were dried at 110 °C in air for 1 h, followed by a careful reduction with a stream of 5 vol% $H_2$/Ar at 350 °C for 2 h. The resulting Au/$ZrO_2$ sample has a specific surface area of ca. 113 $m^2\ g^{-1}$ and a gold concentration of 0.8% by weight.

**Preparation of Au/$ZrO_2$ NCs Catalyst.** Results from previous studies[27] show that the size of the gold particles, an essential requirement for attaining active catalysts, is critically dependent on a number of parameters including the preparation methods, the choice of support, and, in particular, the conditions used for catalyst preparation. Focusing on the preparation parameters that influence the Au particle size in Au/$ZrO_2$ samples prepared by the modified DP procedure as described above, we have been able to prepare a new generation of Au catalyst with a much smaller gold size than that of the Au/$ZrO_2$ catalyst by decreasing the initial concentration of the $HAuCl_4$ stock solution and an optimization of the thermal activation conditions. Basically, an appropriate amount of $ZrO_2$ powder was added to the aqueous solution of $HAuCl_4$ (0.25 mM),and the pH of which was adjusted to 9.0 with 0.25 M $NH_4OH$ under stirring. The aqueous dispersion was stirred for 8 h at 25 °C, while the pH was maintained constantly on 9.0 and then filtered. Extensive washing with deionized water was then followed until it was free of chloride ions. The sample was dried under vacuum at 25 °C for 12 h, followed by a careful reduction with a stream of 5 vol% $H_2$/Ar at 250 °C for 2 h. The resulting sample, containing 0.8 wt % Au as determined by ICP-AES, is denoted as Au/$ZrO_2$ NCs, which has a specific surface area of ca. 114 $m^2\ g^{-1}$.

**Decomposition of FA in an Open System.** All catalytic experiments were carried out under ambient atmosphere of air. It should be noted that the use of inert atmosphere ($N_2$) gave essentially the same rate of $H_2$ evolution as air in this reaction. All reactions, unless otherwise stated, were performed in a double-walled thermostatically controlled reaction vessel (10 mL) under steady magnetic stirring (800 rpm) at a given temperature (25−50 °C) with a reflux condenser, which is connected to an automatic gas buret, where the gases are collected (temperature kept constant at 25 °C during measurements). The gas buret is equipped with a pressure sensor. Evolving gas during the reaction causes a pressure increase in the closed system, which is compensated by volume increase of the buret syringe by an automatic controlling unit. The gas evolution curves are collected by a personal computer. There is a two piston buret for measurements above 100 mL. In addition, evolved gas was qualitatively and quantitatively analyzed by GC (Agilent 6820 equipped with a TDX-01 column connected to a thermal conductivity detector). Typically a ratio of hydrogen and carbon dioxide of 1:1 (±5%) is detected.

**Reuse of Au/$ZrO_2$ NCs Catalyst for Decomposition of TEAF.** For the catalyst reuse experiment, the centrifuged catalysts from parallel activity tests were collected and washed with deionized water, followed by drying under vacuum at room temperature for 12 h and reduction with a stream of 5 vol% $H_2$/Ar at 250 °C for 2 h. All catalytic activity tests were carried out by following the same procedure as described in the Decomposition of FA in an Open System Section. To verify whether there is any leaching of gold or zirconia during the catalytic FA decomposition (Table 1, entry 5), the Au/$ZrO_2$ NC was removed from the reaction mixture by filtration after 3 h reaction.


dx.doi.org/10.1021/ja301696e | J. Am. Chem. Soc. 2012, 134, 8926−8933

Analysis of the filtrate by ICP-AES showed no detectable leaching of Au or Zr (<2.5 ppb) into the solution.

**Pressurized $H_2$ Generation in a Closed System.** The catalytic experiment was carried out in a Hastelloy-C high-pressure Parr autoclave (50 mL). Typically, 5.0 mL scale of adducts including 53.0 mmol FA, 21.2 mmol $NEt_3$, and 30.0 $\mu$mol Au ($Au/ZrO_2$ NCs), was placed in the autoclave. Then the autoclave was sealed, and the internal air was degassed quickly and completely using $N_2$ at room temperature. The stirrer was started (800 rpm) when the desired temperature of 40 °C was reached.

**Continuous $H_2$ Generation Using the $Au/ZrO_2$ NCs TEAF System.** A 50 mL Hastelloy-C high-pressure Parr autoclave with a modified output valve that allows the control of the gas outflow is connected to a high-pressure pump (Waters 1525 binary pump for FA feeding) and to a mass flow controller (MFC, Brooks). Initially a mixture of 4.0 mL FA and 6.0 mL $NEt_3$ was placed in the autoclave reactor containing 7.5 $\mu$mol Au catalyst (187 mg $Au/ZrO_2$ NCs). The reaction temperature was controlled internally. The stirrer was started (800 rpm) until the desired temperature of 50 °C was reached. Once the initial amount of FA had reacted, continuous addition of FA (ca. 0.34 mL $h^{-1}$) was started, and the gas was released at a rate (148 L $H_2$ $h^{-1}$ $g_{Au}{}^{-1}$), thus the pressure inside the autoclave could be maintained at a constant value of ca. 2.0 MPa. As shown in Figure 2, the output rate of evolved hydrogen gas was about 1.18 L $h^{-1}$ $g_{cat}{}^{-1}$ at 50 °C during 100 h. Thus, with 0.5−2.0 g of present $Au/ZrO_2$ NC catalyst, 0.59−2.36 L $H_2$ $h^{-1}$ can be generated.[9] Taking a fuel cell operation efficiency of ca. 60% into consideration, this gives an energy output after the small proton exchange membrane (PEM) fuel cell of ∼0.5−2.0 Wh, which can operate small devices, such as cell phones and toys, etc.

**KIE Experiments.** All experiments were carried out by following the same procedure as described in Decomposition of FA in an Open System Section. The various deuterium-labeled FA and $NEt_3$ were purified by anhydrous $CuSO_4$. The isotope distribution for evolved hydrogen gas was carried out by dividing the reactor effluent into two parallel streams: one was analyzed with a mass spectrometer (Balzers OmniStar) and the other with a gas chromatograph Agilent 6820 equipped with a TDX-01 column connected to a thermal conductivity detector. Typically a ratio of hydrogen ($H_2$ or HD or $D_2$) and carbon dioxide of 1:1 (±5%) is detected.

**CO Oxidation.** The catalytic activity test for CO oxidation was evaluated at atmospheric pressure using a fixed bed quartz reactor (i.d. 3 mm). The weight of the catalyst was 62.5 mg, and the total flow rate of the reaction gas was 37 mL $min^{-1}$, with a composition of 1 vol% CO−20 vol% $O_2$ balanced with He. Kinetic data were collected after 90 min reaction at 25 °C. The composition of the influent and effluent gas was detected with an online gas chromatograph (TCD) equipped with a TDX-01 column. The conversion of CO was calculated from the change in CO concentrations of the inlet and outlet gases.

**WGS Reaction.** WGS reaction was carried out at atmospheric pressure using a fixed bed quartz reactor (i.d. 3 mm). The weight of the catalyst was 100 mg, and the total flow rate of the reaction gas was 100 mL $min^{-1}$, with a composition of 1 vol% CO−4 vol% $H_2O$ (bubbling at 30 °C) balanced with He. Kinetic data were collected after 90 min reaction at 150 °C. The composition of the influent and effluent gas was detected with an online gas chromatograph (TCD) equipped with a TDX-01 column. The conversion of CO was calculated from the change in CO concentrations of the inlet and outlet gases.

**In situ FTIR Measurements.** In situ FTIR measurements were carried out in a Harrick diffuse reflectance infrared cell with $CaF_2$ windows and adapted to the FTIR spectrometer (Nicolet FTIR/R760). Spectra were obtained on the apparatus loaded with 50 mg of catalyst recording at 4 $cm^{-1}$ resolution with 128 scans. Prior to the adsorption of HCOOD (bubbled with He at 10 °C, 20 mL $min^{-1}$, HCOOD content was ∼2%), sample was subjected to the pretreatment with He flow at 200 °C for removing any other gases and moisture. Each spectrum was obtained under the treatment with He flow at indicated temperature and evacuated time and by subtracting the relevant background (base spectrum) of the unloaded sample.

## ■ ASSOCIATED CONTENT

### Ⓢ Supporting Information

Chemicals and materials, catalyst characterization, preparation of other catalysts, and the supplementary results. This material is available free of charge via the Internet at http://pubs.acs.org.

## ■ AUTHOR INFORMATION

### Corresponding Author

yongcao@fudan.edu.cn

### Notes

The authors declare no competing financial interest.

## ■ ACKNOWLEDGMENTS

Financial support by the National Natural Science Foundation of China (20873026, 20803012, and 21073042), New Century Excellent Talents in the University of China (NCET-09-0305), the State Key Basic Research Program of PRC (2009CB623506), and Science & Technology Commission of Shanghai Municipality (08DZ2270500) is kindly acknowledged. The authors are also grateful to Prof. Jian-Qiang Wang from the Shanghai Synchrotron Radiation Facility, Shanghai Institute of Applied Physics, Chinese Academy of Sciences, for the EXAFS analysis.

## ■ REFERENCES

(1) (a) *International energy outlook*; U.S. Energy Information Administration (EIA), U.S. Department of Energy: Washington, D.C., 2010; http://www.eia.gov/forecasts/ieo/index.cfm. (b) Enthaler, S. *ChemSusChem* **2008**, *1*, 801. (c) Joó, F. *ChemSusChem* **2008**, *1*, 805. (d) Jiang, H. L.; Singh, S. K.; Yan, J. M.; Zhang, X. B.; Xu, Q. *ChemSusChem* **2010**, *3*, 541. (e) Yu, K. M. K.; Curcic, I.; Gabriel, J.; Tsang, S. C. E. *ChemSusChem* **2008**, *1*, 893.

(2) (a) Schlapbach, L.; Züttel, A. *Nature* **2001**, *414*, 353. (b) Huber, G. W.; Iborra, S.; Corma, A. *Chem. Rev.* **2006**, *106*, 4044. (c) Navarro, R. M.; Peña, M. A.; Fierro, J. L. G. *Chem. Rev.* **2007**, *107*, 3952. (d) Staubitz, A.; Robertson, A. P. M.; Manners, I. *Chem. Rev.* **2010**, *110*, 4079.

(3) (a) Boddien, A.; Gärtner, F.; Federsel, C.; Sponholz, P.; Mellmann, D.; Jackstell, R.; Junge, H.; Beller, M. *Angew. Chem., Int. Ed.* **2011**, *50*, 6411. (b) Schaub, T.; Paciello, R. A. *Angew. Chem., Int. Ed.* **2011**, *50*, 7278. (c) Preti, D.; Resta, C.; Squarcialupi, S.; Fachinetti, G. *Angew. Chem., Int. Ed.* **2011**, *50*, 12551. (d) Johnson, T. C.; Morris, D. J.; Wills, M. *Chem. Soc. Rev.* **2010**, *39*, 81. (e) Majewski, A.; Morris, D. J.; Kendall, K.; Wills, M. *ChemSusChem* **2010**, *3*, 431.

(4) (a) *Fuel Cells Technologies Program Multi-Year Research, Development and Demonstration Plan*, Planned program activities for 2005−2015. Technical Plan−Fuel Cells; U.S. Department of Energy: Washington, D.C.; http://www1.eere.energy.gov/hydrogenandfuelcells/mypp/. (b) Kim, Y. H.; Park, E. D.; Lee, H. C.; Lee, D. *Appl. Catal. A: Gen.* **2009**, *366*, 363.

(5) (a) Wu, X.; Li, X.; King, F.; Xiao, J. *Angew. Chem., Int. Ed.* **2005**, *44*, 3407. (b) Matharu, D. S.; Morris, D. J.; Clarkson, G. J.; Wills, M. *Chem. Commun.* **2006**, *30*, 3232. (c) Loges, B.; Boddien, A.; Gärtner, F.; Junge, H.; Beller, M. *Top. Catal.* **2010**, *53*, 902. (d) Wienhöfer, G.; Sorribes, I.; Boddien, A.; Westerhaus, F.; Junge, K.; Junge, H.; Llusar, R.; Beller, M. *J. Am. Chem. Soc.* **2011**, *133*, 12875.

(6) (a) Loges, B.; Boddien, A.; Junge, H.; Beller, M. *Angew. Chem., Int. Ed.* **2008**, *47*, 3962. (b) Boddien, A.; Loges, B.; Junge, H.; Beller, M. *ChemSusChem* **2008**, *1*, 751. (c) Boddien, A.; Loges, B.; Junge, H.; Gärtner, F.; Noyes, J. R.; Beller, M. *Adv. Synth. Catal.* **2009**, *351*, 2517. (d) Junge, H.; Boddien, A.; Capitta, F.; Loges, B.; Noyes, J. R.; Gladiali, S.; Beller, M. *Tetrahedron Lett.* **2009**, *50*, 1603.

(7) (a) Fellay, C.; Dyson, P. J.; Laurenczy, G. *Angew. Chem., Int. Ed.* **2008**, *47*, 3966. (b) Fellay, C.; Yan, N.; Dyson, P. J.; Laurenczy, G. *Chem.—Eur. J.* **2009**, *15*, 3752.

(8) Boddien, A.; Mellmann, D.; Gärtner, F.; Jackstell, R.; Junge, H.; Dyson, P. J.; Laurenczy, G.; Ludwig, R.; Beller, M. *Science* **2011**, *333*, 1733.
(9) Tedsree, K.; Li, T.; Jones, S.; Chan, C. W. A.; Yu, K. M. K.; Bagot, P. A. J.; Marquis, E. A.; Smith, G. D. W.; Tsang, S. C. E. *Nat. Nanotechnol.* **2011**, *6*, 302.
(10) (a) Sabatier, P.; Mailhe, A. *C. R. Acad. Sci.* **1911**, *152*, 1212. (b) Iglesia, E.; Boudart, M. *J. Catal.* **1983**, *81*, 214. (c) Barteau, M. A. *Catal. Lett.* **1991**, *8*, 175. (d) Solymosi, F.; Koós, Á.; Liliom, N.; Ugrai, I. *J. Catal.* **2011**, *279*, 213. (e) Tedsree, K.; Kong, A. T. S.; Tsang, S. C. *Angew. Chem., Int. Ed.* **2009**, *48*, 1443. (f) Tedsree, K.; Chan, C. W. A.; Jones, S.; Cuan, Q.; Li, W. K.; Gong, X. Q.; Tsang, S. C. E. *Science* **2011**, *332*, 224. (g) Ojeda, M.; Iglesia, E. *Angew. Chem., Int. Ed.* **2009**, *48*, 4800.
(11) (a) Zhou, X.; Huang, Y.; Xing, W.; Liu, C.; Liao, J.; Lu, T. *Chem. Commun.* **2008**, *30*, 3540. (b) Gu, X. J.; Lu, Z. H.; Jiang, H. L.; Akita, T.; Xu, Q. *J. Am. Chem. Soc.* **2011**, *133*, 11822. (c) Zhao, Y.; Deng, L.; Tang, S. Y.; Lai, D. M.; Liao, B.; Fu, Y.; Guo, Q. X. *Energy Fuels* **2011**, *25*, 3693.
(12) (a) Zhang, X.; Xamena, F. X. L.; Corma, A. *J. Catal.* **2009**, *265*, 155. (b) Tsunoyama, H.; Liu, Y. M.; Akita, T.; Ichikuni, N.; Sakurai, H.; Xie, S. H.; Tsukuda, T. *Catal. Surv. Asia* **2011**, *15*, 230. (c) Liu, Y. M.; Tsunoyama, H.; Akita, T.; Xie, S. H.; Tsukuda, T. *ACS Catal.* **2011**, *1*, 2. (d) Comotti, M.; Pina, C. D.; Matarrese, R.; Rossi, M. *Angew. Chem., Int. Ed.* **2004**, *43*, 5812. (e) Corma, A.; Serna, P. *Science* **2006**, *313*, 332. (f) Ishida, T.; Haruta, M. *Angew. Chem., Int. Ed.* **2007**, *46*, 7154. (g) Wittstock, A.; Zielasek, V.; Biener, J.; Friend, C. M.; Bäumer, M. *Science* **2010**, *327*, 319. (h) Zhu, Y.; Qian, H.; Drake, B. A.; Jin, R. *Angew. Chem., Int. Ed.* **2010**, *49*, 1295. (i) Rodriguez, J. A.; Ma, S.; Liu, P.; Hrbek, J.; Evans, J.; Pérez, M. *Science* **2007**, *318*, 1757. (j) Kim, D. Y.; Yu, T.; Cho, E. C.; Ma, Y.; Park, O. O.; Xia, Y. *Angew. Chem., Int. Ed.* **2011**, *50*, 6328. (k) Su, F. Z.; Liu, Y. M.; Wang, L. C.; Cao, Y.; He, H. Y.; Fan, K. N. *Angew. Chem., Int. Ed.* **2008**, *47*, 334. (l) Sun, H.; Su, F. Z.; Ni, J.; Cao, Y.; He, H. Y.; Fan, K. N. *Angew. Chem., Int. Ed.* **2009**, *48*, 4390. (m) He, L.; Wang, L. C.; Sun, H.; Ni, J.; Cao, Y.; He, H. Y.; Fan, K. N. *Angew. Chem., Int. Ed.* **2009**, *48*, 9538.
(13) Du, X. L.; He, L.; Zhao, S.; Liu, Y. M.; Cao, Y.; He, H. Y.; Fan, K. N. *Angew. Chem., Int. Ed.* **2011**, *50*, 7815.
(14) Himeda, Y. *Green Chem.* **2009**, *11*, 2018.
(15) (a) Boddien, A.; Loges, B.; Gärtner, F.; Torborg, C.; Fumino, K.; Junge, H.; Ludwig, R.; Beller, M. *J. Am. Chem. Soc.* **2010**, *132*, 8924. (b) Boddien, A.; Gärtner, F.; Jackstell, R.; Junge, H.; Spannenberg, A.; Baumann, W.; Ludwig, R.; Beller, M. *Angew. Chem., Int. Ed.* **2010**, *49*, 8993.
(16) It should be emphasized that there was no leaching of gold or $ZrO_2$ under such highly acidic conditions, verifying the inherent stability of the $Au/ZrO_2$ NCs catalyst in strong acidic media. See the Supporting Information for details.
(17) Enthaler, S.; Langermann, J.; Schmidt, T. *Energy Environ. Sci.* **2010**, *3*, 1207.
(18) Flipsen, B. *J. Fuel Cell Sci. Technol.* **2010**, *7*, 061014−1.
(19) (a) Fukuzumi, S.; Kobayashi, T.; Suenobu, T. *ChemSusChem* **2008**, *1*, 827. (b) Fukuzumi, S.; Kobayashi, T.; Suenobu, T. *J. Am. Chem. Soc.* **2010**, *132*, 1496. (c) Hauwert, P.; Boerleider, R.; Warsink, S.; Weigand, J. J.; Elsevier, C. J. *J. Am. Chem. Soc.* **2010**, *132*, 16900.
(20) It is important to remark that, based on the XPS data, there is only metallic $Au^0$ on the surface of $Au/ZrO_2$ NCs sample. Note that the presence of various amount of cationic Au species over different supported gold catalysts has been reported elsewhere (see refs 12a and b), which may be affected by a number of factors, such as the properties of supports, preparing methods, and so forth. Detailed description about this issue is beyond the scope of this study.
(21) Siani, A.; Alexeev, O. S.; Deutsch, D. S.; Monnier, J. R.; Fanson, P. T.; Hirata, H.; Matsumoto, S.; Williams, C. T.; Amiridis, M. D. *J. Catal.* **2009**, *266*, 331.
(22) (a) Menegazzo, F.; Manzoli, M.; Chiorino, A.; Boccuzzi, F.; Tabakova, T.; Signoretto, M.; Pinna, F.; Pernicone, N. *J. Catal.* **2006**, *237*, 431. (b) Menegazzo, F.; Pinna, F.; Signoretto, M.; Trevisan, V.; Boccuzzi, F.; Chiorino, A.; Manzoli, M. *Appl. Catal. A: Gen.* **2009**, *356*, 31.
(23) We would like to emphasize here that, bearing essentially the same underlying support, the decreased activity of $Au/ZrO_2$ NCs relative to that of $Au/ZrO_2$ for CO oxidation is attributable to a stronger adsorption of CO as a result of the decreased size of the Au particles or clusters (see Figure S9, Supporting Information). In the specific field of CO oxidation, the essential role of zirconia as a support for gold is believed to provide oxygen adsorption and activation sites, possibly the oxygen vacancies or reactive perimeter sites at $Au-ZrO_2$ interface, which in turn can afford large amount of highly mobile oxygen species being able to react with CO. See: Widmann, D.; Liu, Y.; Schüth, F.; Behm, R. J. *J. Catal.* **2010**, *276*, 292.
(24) (a) Valden, M.; Lai, X.; Goodman, D. W. *Science* **1998**, *281*, 1647. (b) Bond, G. C.; Thompson, D. T. *Gold Bull.* **2000**, *33*, 44. (c) Daté, M.; Okukura, M.; Tsubota, S.; Haruta, M. *Angew. Chem., Int. Ed.* **2004**, *43*, 2129. (d) Liu, Y.; Jia, C. J.; Yamasaki, J.; Terasaki, O.; Schüth, F. *Angew. Chem., Int. Ed.* **2010**, *49*, 5771.
(25) (a) Ross-Medgaarden, E. I.; Knowles, W. V.; Kim, T.; Wong, M. S.; Zhou, W.; Kiely, C. J.; Wachs, I. E. *J. Catal.* **2008**, *256*, 108. (b) Graf, P. O.; Vlieger, D. J. M.; Mojet, B. L.; Lefferts, L. *J. Catal.* **2009**, *262*, 181. (c) Postole, G.; Chowdhury, B.; Karmakar, B.; Pinki, K.; Banerji, J.; Auroux, A. *J. Catal.* **2010**, *269*, 110.
(26) (a) Chiorino, A.; Manzoli, M.; Menegazzo, F.; Signoretto, M.; Vindigni, F.; Pinna, F.; Boccuzzi, F. *J. Catal.* **2009**, *262*, 169. (b) Azizi, Y.; Petit, C.; Pitchon, V. *J. Catal.* **2010**, *269*, 26.
(27) Fang, W. H.; Chen, J. S.; Zhang, Q. H.; Deng, W. P.; Wang, Y. *Chem.—Eur. J.* **2011**, *17*, 1247.